

**Disruption of the cytoplasmic membrane structure and barrier function underlines the potent antiseptic activity of octenidine in Gram-positive bacteria**

Nermina Malanovic<sup>1#</sup>, Jessica A. Buttress<sup>3</sup>, Djenana Vejzovic<sup>1</sup>, Ayse Ön<sup>1</sup>, Paulina Piller<sup>1</sup>, Dagmar Kolb<sup>2,4</sup>, Karl Lohner<sup>1,2</sup> and Henrik Strahl<sup>3</sup>

<sup>1</sup>Institute of Molecular Biosciences, Biophysics Division, University of Graz, NAWI Graz, Graz, Austria

<sup>2</sup>Bio TechMed Graz, 8010 Graz, Austria

<sup>3</sup>Centre for Bacterial Cell Biology, Biosciences Institute, Faculty of Medical Sciences, Newcastle University, Baddiley-Clark Building, Richardson Road, Newcastle upon Tyne, NE2 4AX, United Kingdom

<sup>4</sup>Core Facility Ultrastructure Analysis, Center for Medical Research, Medical University of Graz, Stiftingtalstrasse 24, 8010 Graz, Austria

\* djenana.vejzovic@hotmail.com

§ ayse\_oen@hotmail.com

#Corresponding author:

email: [nermina.malanovic@uni-graz.at](mailto:nermina.malanovic@uni-graz.at)

Institute of Molecular Biosciences, Biophysics Division, University of Graz, Humboldtstrasse 50/III, 8010 Graz, Austria.

Running title: Antimicrobial mode of action of octenidine

## 1 **Supplementary Methods**

2 A set of experiments were performed in analogy to our previous work [1].

3

### 4 **Electron microscopy**

5 Electron microscopy was carried out with the same workflow and set up we used for *E. coli* and  
6 published before [1]. Samples were prepared with  $2.5 \times 10^8$  CFU/ml *E. hirae* from the mid-  
7 logarithmic culture and incubated for 30 min at 37°C in presence of below (0.0001 %), at  
8 (0.0004 %) and above the lethal concentration (0.001 %) of OCT. Experiments were performed  
9 twice and images were taken of at least six cuts of which representative once are shown.

10

### 11 **Zeta potential and vesicle size measurements**

12 Mid-logarithmic *E. hirae/B. subtilis* cultures were diluted to  $1 \times 10^7$  CFU/ml in HEPES buffer  
13 (10 mM HEPES, 140 mM NaCl, pH 7.4) and incubated with OCT from  $1 \times 10^{-9}$  to  $1 \times 10^{-3}$ % (5  
14 min, room temperature) before measuring the samples in a Zetasizer NANO (Malvern  
15 Instruments, Germany) according to methods published previously [1,2].

16

### 17 **Flow cytometry**

18 600-1200  $\mu$ l of the  $1 \times 10^6$  CFU/ml cell suspension were incubated for 5 min at room temperature  
19 with 1  $\mu$ g/ml propidium iodide (PI) in the dark. PI fluorescence was measured with BD LSR  
20 Fortessa™ in real-time using the BD FACS Diva Software. Signals from side and forward  
21 scatter were also collected, as they relate to complexity and cell size of bacteria. After 30 sec,  
22 OCT in several dilutions from 0.00005 to 0.001 % was added to the labelled bacterial cells,  
23 mixed and fluorescence of PI was followed for 5-20 min. We used the membrane-active  
24 antimicrobial peptide SAAP-148 [3] as a positive control, which is known to permeabilise

25 bacterial membranes. FACS experiments in the presence of OCT were repeated in the absence  
26 of PI.

27

### 28 **Fluorescence microscopy (*E. hirae*)**

29 Assays for *E. hirae* were performed as described previously [1,4]. A mid-logarithmic growth-  
30 phase culture of *E. hirae* was diluted in PBS to  $2.5 \times 10^8$  CFU/ml. 200  $\mu$ l of this cell suspension  
31 was incubated with OCT concentrations below (0.0001 %), at (0.0004 %) and above (0.001 %) the  
32 lethal concentration (20 min; 37°C; 300 rpm) before they were stained with 10  $\mu$ g/ml of the  
33 fluorescent membrane dye Nile Red. The used microscope and set-up was according to  
34 Wolinski *et al.* [5]. Nile Red was excited at 561 nm and fluorescence emission was detected  
35 between 570-750 nm.

36

### 37 **Vesicle leakage assay**

38 For leakage experiments, large unilamellar vesicles composed of POPE, POPG, POPE/TOCL  
39 (80:10 mol), POPG/TOCL (80:20 mol), POPE/POPG/TMCL (6:2:1 mol) or *E. coli* polar lipid  
40 extract (PE 67 %, PG 23.2 % and CL 9.8 %) were prepared in 10 mM HEPES buffer pH 7.4  
41 containing 68 mM NaCl, 12.5 mM ANTS and 45 mM DPX. Leakage of the aqueous content of  
42 the 50  $\mu$ M ANTS/DPX loaded lipid vesicles upon incubation with OCT-to-lipid molar ratios  
43 from 1:25 to 1:1.5 was determined as described previously [1]. Fluorescence emission was  
44 recorded at 37°C as a function of time before and after the addition of OCT. Triton was used as  
45 a positive control for maximum induced leakage of fluorescent dye.

46

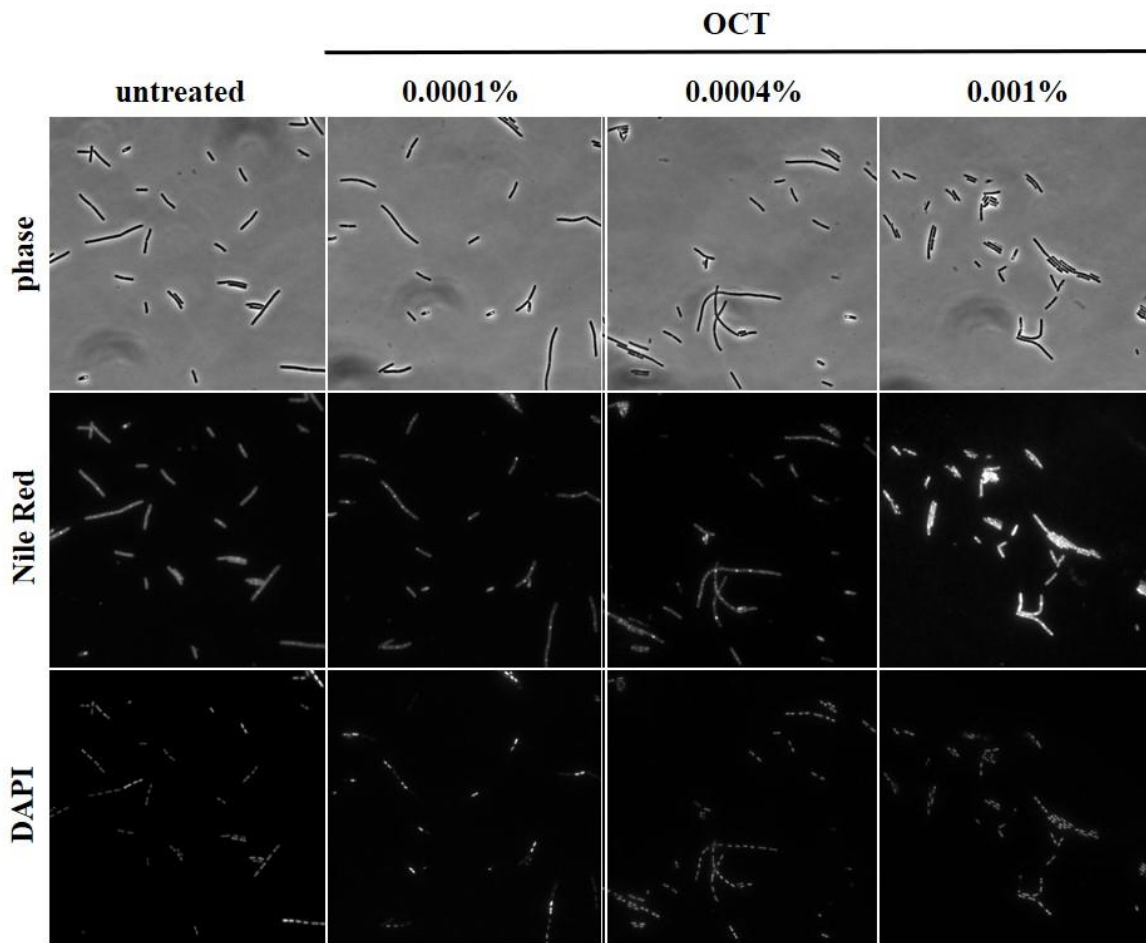
### 47 **Differential Scanning Calorimetry (DSC)**

48 Calorimetric measurements were performed using a Microcal VP-DSC high-sensitivity  
49 differential scanning calorimeter (Microcal, USA) or Nano DSC (TA Instruments, Germany)

50 as described before [6]. DSC measurements were carried out in presence and absence of OCT  
51 on model membranes composed of major phospholipids (DMPG, TMCL and DMPG/TMCL  
52 mixture (80:20 molar) of the Gram-positive membranes [7]. Total lipid concentration was 1  
53 mg/ml and the used OCT concentration was calculated to correspond to a lipid-to-OCT molar  
54 ratio of 6:1. Preparation of the model membranes was done as described before [6].

55 **Supplementary Figures**

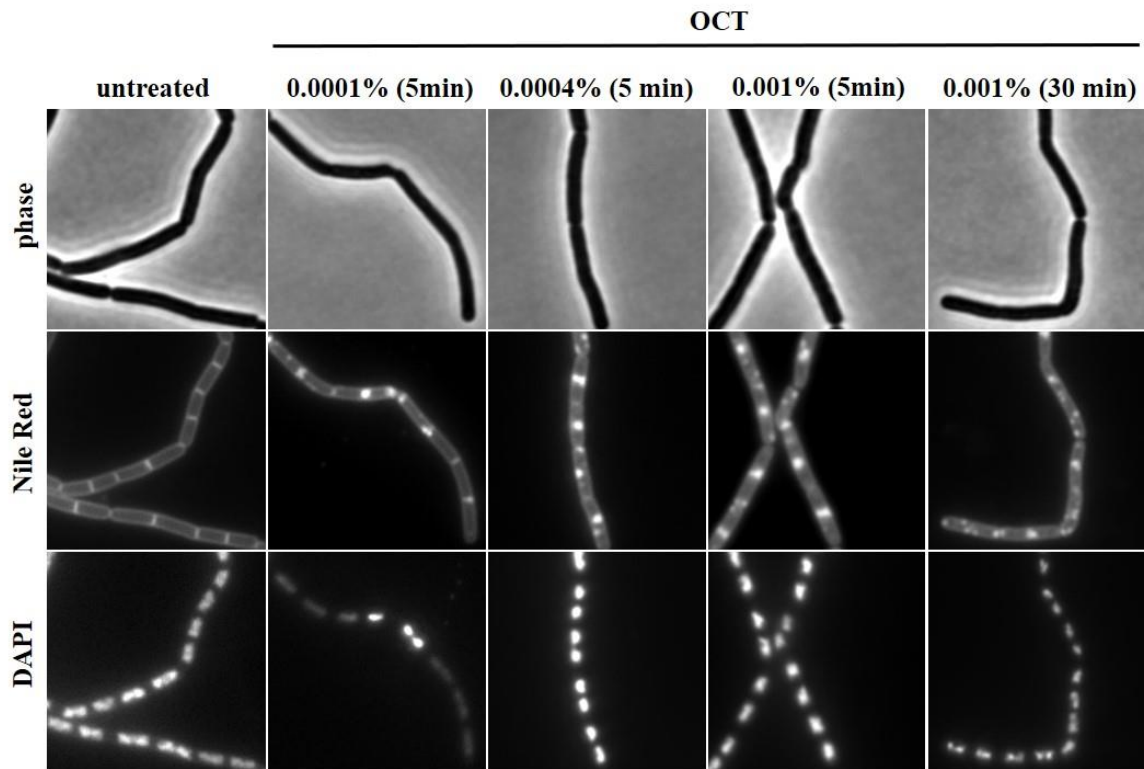
56



57

58 **Supplementary Figure S1: OCT disturbs membrane organisation and fluidity in *B.***  
59 ***subtilis*; a larger field of view.**

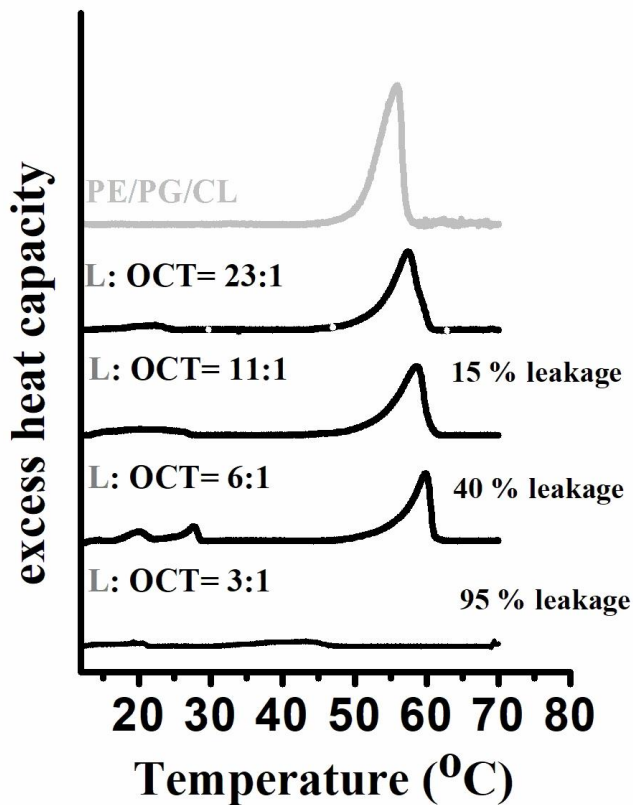
60 Phase contrast and fluorescent microscopy images of *B. subtilis* cells co-stained with the  
61 membrane dye Nile Red and the DNA dye DAPI, in the absence and presence of different  
62 concentrations of OCT (5 min). These images show a larger field of view with more cells of  
63 the data show in Figure 7. Strain used: *B. subtilis* 168 (wild type).



64

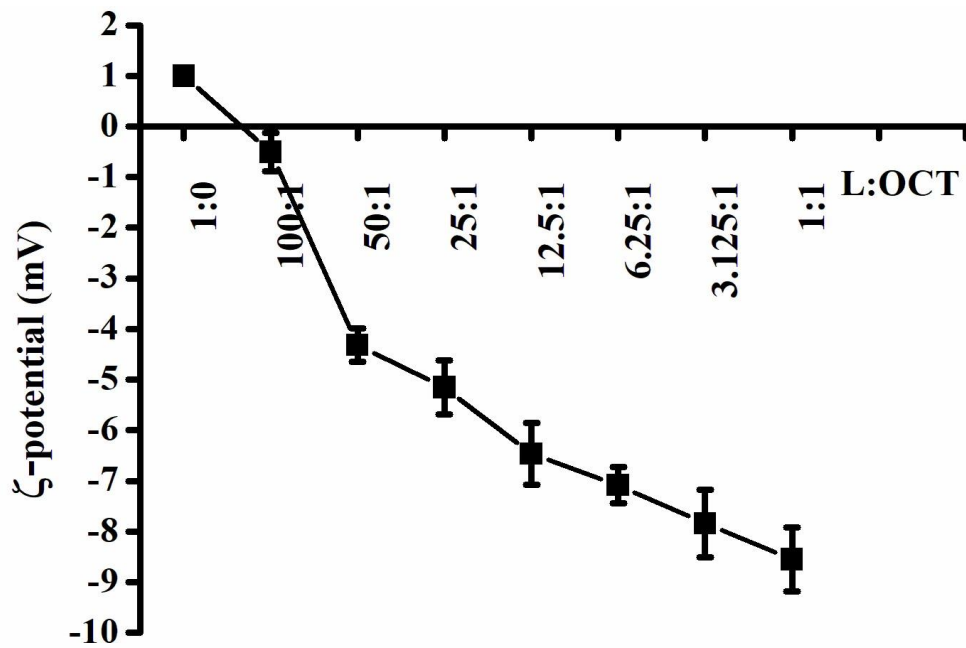
65 **Supplementary Figure S2: Weakly Nile Red-stained membrane areas are a**  
 66 **manifestation of cell lysis.**

67 Phase contrast and fluorescent microscopy images of *B. subtilis* cells deficient for cell wall  
 68 autolytic enzymes LytC-F, co-stained with the membrane dye Nile Red and the DNA dye DAPI,  
 69 and incubated in the absence and presence of different concentrations of OCT (5-30 min). Note  
 70 the lack of weakly stained membrane areas observed in lysing wild type cells whilst the brightly  
 71 stained foci associated with membrane invaginations are still present. Strain used: *B. subtilis*  
 72 KS19 ( $\Delta$ *lytABCDEF*). Due to the lack of cell wall hydrolase activity, these cells exhibit a chainy  
 73 cell morphology as they cannot complete septal cleavage.



74

75 **Supplementary Figure S3. OCT affects membrane properties of PE/PG/CL membrane**  
 76 **models as determined by calorimetric measurements.** Thermodynamic studies of PE/PG/CL  
 77 mixture (grey line) in the presence of indicated OCT concentration (black lines). Heating scans  
 78 of PE/ PG/CL model membranes as observed at the indicated molar lipid-to-OCT ratios. Scan  
 79 rate was 30°C/h. Data are representative examples of at least two independent experiments



80

81 **Supplementary Figure S4. OCT neutralizes surface charge of the PE membranes.**

82 Measurement of zeta potential of 50  $\mu$ M PE in absence and presence of 0.5-50  $\mu$ M OCT.

83 Samples were incubated for 5 min before analysis. Results were performed in duplicates of 30

84 independent calculations measured at least two times.



## 85 **Supplementary References**

- 86 [1] Malanovic N, Ön A, Pabst G, Zellner A, Lohner K. Octenidine: Novel insights into  
87 the detailed killing mechanism of Gram-negative bacteria at a cellular and molecular  
88 level. *Int J Antimicrob Agents* 2020;56:106146.
- 89 [2] Pérez-Peinado C, Dias SA, Domingues MM, Benfield AH, Freire JM, Rádis-  
90 Baptista G, Gaspar D, Castanho MARB, Craik DJ, Henriques ST, Veiga AS,  
91 Andreu D. Mechanisms of bacterial membrane permeabilization by crotalidicin (Ctn)  
92 and its fragment Ctn(15-34), antimicrobial peptides from rattlesnake venom, *J Biol*  
93 *Chem* 2018;293:1536-1549.
- 94 [3] de Breij A, Riool M, Cordfunke RA, Malanovic N, de Boer L, Koning RI,  
95 Ravensbergen E, Franken M, van der Heijde T, Boekema BK, Kwakman PHS,  
96 Kamp N, El Ghalbzouri A, Lohner K, Zaat SAJ, Drijfhout JW, Nibbering PH. The  
97 antimicrobial peptide SAAP-148 combats drug-resistant bacteria and biofilms, *Sci*  
98 *Tranls Med* 2018;10(423):eaa4044
- 99 [4] Scheinpflug K, Krylova O, Nikolenko H, Thurm C, Dathe M. Evidence for a novel  
100 mechanism of antimicrobial action of a cyclic R-,W-rich hexapeptide, *PLoS One*  
101 2015;e0125056.
- 102 [5] Wolinski H, Kohlwein SD. Microscopic and spectroscopic techniques to investigate  
103 lipid droplet formation and turnover in yeast, *Methods Mol Biol (Clifton, N.J.)*  
104 2015;1270:289-305.
- 105 [6] Malanovic N, Leber R, Schmuck M, Kriechbaum M, Cordfunke RA, Drijfhout JW, de  
106 Breij A, Nibbering PH, Kolb D, Lohner K. Phospholipid-driven differences determine  
107 the action of the synthetic antimicrobial peptide OP-145 on Gram-positive bacterial and  
108 mammalian membrane model systems, *Biochim Biophys Acta* 2015;1848:2437-2447.
- 109 [7] Malanovic N, Lohner K. Gram-positive bacterial cell envelopes. The impact on the  
110 activity of antimicrobial peptides. *Biochim Biophys Acta* 2016;1858:936-946.